HHS Public Access

Author manuscript

J Immunol. Author manuscript; available in PMC 2018 April 01.

Published in final edited form as:

J Immunol. 2017 April 01; 198(7): 2979–2988. doi:10.4049/jimmunol.1601064.

Virus-specific CD8+ T cells infiltrate melanoma lesions and retain function independent of PD-1 expression

Dan A. Erkes[a], **Corinne J. Smith**[a], **Nicole A. Wilski**[a], **Sofia Caldeira-Dantas**[a,b,c], **Toktam Mohgbeli**[a], and **Christopher M. Snyder**[a]

[a]Department of Microbiology and Immunology, Kimmel Cancer Center, Thomas Jefferson University, Philadelphia, PA, USA

[b]Life and Health Sciences Research Institute (ICVS), School of Healthy Sciences, University of Minho, Braga, Portugal

[c]ICVS/3B's, PT Government Associated Laboratory, Braga/Guimarães, Portugal

Abstract

It is well known that $CD8^+$ tumor infiltrating lymphocytes (TIL) are correlated with positive prognoses in cancer patients and used to determine efficacy of immune therapies. While it is generally assumed that $CD8^+$ TIL will be tumor associated antigen (TAA)-specific, it is unknown whether $CD8^+$ T cells with specificity for common pathogens also infiltrate tumors. If so, the presence of these T cells could alter the interpretation of prognostic and diagnostic TIL assays. We compared TAA-specific and virus-specific $CD8^+$ T cells in the same tumors using murine cytomegalovirus (MCMV), a herpesvirus that causes a persistent/latent infection, and Vaccinia virus (VacV), a poxvirus that is cleared by the host. Virus-specific $CD8^+$ TIL migrated into cutaneous melanoma lesions during acute infection with either virus, as well as after a cleared VacV infection, and during a persistent/latent MCMV infection. Virus-specific TILs developed independent of viral antigen in the tumor and interestingly, expressed low or intermediate levels of full-length PD-1 in the tumor environment. Importantly, PD-1 expression could be markedly induced by antigen, but did not correlate with dysfunction for virus-specific TIL, in sharp contrast to TAA-specific TIL in the same tumors. These data suggest that $CD8^+$ TIL can reflect an individual's immune status, rather than exclusively representing TAA-specific T cells, and that PD-1 expression on $CD8^+$ TIL is not always associated with repeated antigen encounter or dysfunction. Thus, functional virus-specific $CD8^+$ TIL could skew the results of prognostic or diagnostic TIL assays.

Introduction

For cancer, there is a strong correlation between the level of tumor infiltrating lymphocytes (TIL), especially $CD8^+$ T cells, and overall patient survival [1, 2]. As many studies have demonstrated that tumor associated antigen (TAA)-specific $CD8^+$ T cells can limit tumor growth [3], strategies have been designed to increase the level of TAA-specific $CD8^+$ TIL

Corresponding Author: **Christopher M. Snyder, PhD**, Thomas Jefferson University, Department of Microbiology and Immunology, Kimmel Cancer Center, 233 S 10th St, BLSB, rm 526, Philadelphia, PA 19107, Tel: 215-503-2543, christopher.snyder@jefferson.edu.

[4–8]. $CD8^+$ TIL are embedded in the tumor tissue and often express an array of inhibitory receptors, such as PD-1 [9–11]. There is a strong correlation between PD-1 expression and T cell exhaustion in TAA-specific $CD8^+$ TIL, defined by loss of cytokine production, cytolytic capacity, and proliferative potential [9–13], which can be rescued upon PD-1/PD-L1 blockade [10]. These observations have led to extensive clinical trials and FDA approval of antibodies that block PD-1/PD-L1 interactions [10, 14].

The recent availability of multiple anti-tumor immune therapies has led to prognostic and diagnostic assays based upon the level of $CD8^+$, $CD8^+/PD\text{-}1^+$, or $CD8^+/IFN\gamma^+$ cells in tumors, blood, and tumor draining lymph nodes of patients [2, 15]. It is often assumed that all T cells present in tumors are TAA-specific. However, little is known about how acute, cleared, or latent infections may affect TIL populations. People are frequently and repeatedly exposed to pathogens that must be controlled by the immune system. Moreover, everyone in the world is infected with multiple persistent viruses such as herpes viruses [16], which require constant immune surveillance for control [17, 18]. Additionally, naïve $CD8^+$ T cells are able to migrate into tumor masses, where they can undergo activation and differentiation [19]. Thus, it is possible that T cell responses to acute, cleared or latent infections may result in infection-specific $CD8^+$ T cells entering tumors. The potential influx of T cells not specific for TAAs, and the immune status of the individual, could greatly affect the prognostic and diagnostic value of TIL assays.

To explore this, we used murine cytomegalovirus (MCMV) and Vaccinia virus (VacV) infections in tumor-bearing mice to compare TAA-specific and virus-specific $CD8^+$ T cells in the same tumor. MCMV is a herpesvirus and a well-established model of human CMV (HCMV), a virus that establishes a persistent/latent infection in most people in the world. HCMV is also being explored as a potential vaccine vector for infectious diseases and cancer [20]. VacV is a poxvirus that was used as a vaccine to eradicate smallpox in humans. We found that virus-specific T cells readily became TIL independent of virus infection of the tumor and expressed PD-1 in the tumor. PD-1 levels correlated with recent exposure to antigen. Unexpectedly, PD-1 expression did not correlate with dysfunction of the anti-viral $CD8^+$ TIL population, in sharp contrast with TAA-specific $CD8^+$ TIL. These data suggest that virus-specific $CD8^+$ TIL are part of the normal TIL population, reflecting an individual's immune status, behaving differently than TAA-specific TILs, and potentially skewing prognostic or diagnostic TIL assays.

Materials and Methods

Mice

C57BL/6J, CD45.1 (B6.SJL-$Ptprc^a Pepc^b$/BoyJ), OT-I transgenic mice (C57BL/6-Tg(Tcra-Tcrb)110Mjb/J), Pmel-I transgenic mice (B6.Cg-*Thy1*$_a$/Cy Tg(TcraTcrb)8Rest/J) mice, and $BRaf^{CA}$, Tyr::CreER and $Pten^{lox4\text{-}5}$ (B6.Cg-Tg(Tyr-cre/ERT2)13Bos/J) mice were purchased from Jackson Laboratory and bred in-house. The Thomas Jefferson University Institutional Animal Care and Use Committee reviewed and approved all protocols.

Tumor cell lines and models

B16F0s (kindly provided by Dr. Vitali Alexeev, Department of Dermatology and Cutaneous Biology, Sidney Kimmel Medical College, or purchased from ATCC) were maintained in DMEM (CellGro) + 1% PenStrep + 10% FBS. For B16F0 tumor implantation, cells were suspended at 1×10^6 cells per ml in HBSS (CellGro) and injected subcutaneously into the dorsal flank in a volume of 100 μl (1×10^5 cells/mouse). Melanomas were induced in the $BRaf^{CA}$, Tyr::CreER and $Pten^{lox4\text{-}5}$, triple transgenic mice with tamoxifan as described [21]. In both models, animals were sacrificed at the time point discussed in figure legends, or when tumor size had exceeded ~100 mm^2 as determined by a 6-inch digital caliper (Neiko), or when tumors had ulcerated, or animals became moribund.

Viruses, infections, and intratumoral peptide administration

$MCMV\text{-}gp100^{S27P}$ (MCMV-gp100), MCMV-SL8, WT-MCMV, and MCMV-K181 have all been previously described and were produced and grown as previously described ([22–24]). VacV expressing ovalbumin (VacV-OVA) was kindly provided by Dr. Laurence C. Eisenlohr (The Children's Hospital of Philadelphia Research Institute and The Perelman School of Medicine at The University of Pennsylvania). The timing of infection and strains of MCMV and VacV used are described in each figure legend. In most cases, mice were infected with 2×10^5 pfu of MCMV or 1×10^6 pfu of VacV in 100 μl of PBS delivered via the intrapertoneal (IP) route in a single injection. However, in Fig 1A–Dmice were infected with 5×10^5 pfu of MCMV by IP and intradermal (ID, 25 μl volume) routes simultaneously. Direct comparisons between infection via the IP route alone or IP/ID routes combined revealed no differences in T cell numbers or function within tumors (not shown). In Figure 1E, mice were infected with 6×10^5 pfu of MCMV-gp100 via the IP route. For the intratumoral (IT) peptide injections performed in Fig. 6, B16F0s were implanted into mice 30 days after infection with WT-MCMV. When tumors were 20mm^2, ~7–10 days post implantation, 1 μg of M38 peptide (Genemed Synthesis Inc) suspended in 1 μL of DMSO, or 1 μL of DMSO alone was delivered IT in 30 μL PBS.

Lymphocyte isolation

Analyses of blood and splenocytes were performed as previously described [25, 26]. For recovery of lymphocytes from tumors, tumor masses were placed in digestion media (1x HBSS [Cellgro], 0.1 mg/ml Collagenase A [Worthington], 60 U/ml DNase I [Roche]) [19] and minced using the gentleMACS™ Octo Dissociator using C Tubes (Miltenyi Biotec). Minced tumors were incubated at 37°C for 30 minutes with continuous rotation, minced again as above, washed twice with T cell media (RPMI 1640 [Cellgro] with L-glutamine + 10% FBS + 1% PenStrep and 5×10^{-5} M β-mercaptoethanol [Omnipur, Calbiochem]), and filtered through a 70 μm nylon filter. In most experiments, lymphocytes were then either directly assessed by flow cytometry or tested for their ability to produce cytokines upon stimulation. In some experiments (Fig. 6 A–C, and Supplemental Fig 3A), lymphocytes were enriched from tumor homogenates by spinning through a 40%/80% Percoll (GE Lifesciences) gradient for 25 minutes at 600 × g and collecting cells at the interface. For Supplemental Fig. 3A$CD8^+$ T cells were further enriched with a biotin selection kit and magnetic beads (EasySep, StemCell Technologies) and biotinylated antibodies specific for

NK1.1 (clone PK136), TER-119 (clone TER-119), CD4 (clone GK1.5), and CD19 (clone 6D5), all from Biolegend. Enriched cells were ~80% $CD8^+$.

Flow Cytometry

Intravenous (IV) labeling of T cells to distinguish tissue and vascular-localized cells was performed as previously described [26]. MHC tetramers were provided by the National Institutes of Health Tetramer Core Facility (http://tetramer.yerkes.emory.edu) and used as previously described [25]. Antibodies used for analyses included: CD8α (clone 53.6.7), CD8β (clone YTS156.7.7), PD-1 (clone 29F.1A12), IFN-γ (clone XMG1.2), TNF-α (clone MP6-XT22), CD107a (clone 1D4B), Thy1.1 (clone OX-7), CD45.1 (clone A20), CD45.2 (clone 104), and Vα2 (clone B20.1). All antibodies were purchased from Biolegend. For analysis of PD-L1/PD-L2 binding to T cells (Fig. 6C), lymphocytes were isolated from tumors with Percoll as described above and treated with TruStain FcX (Biolegend) at 1 μg/10^6 cells followed by 1 μg of recombinant PD-L1-Fc or PD-L2-Fc (not shown) chimera proteins at 1 μg/10^6 cells for one hour at room temperature. Cells were washed and stained with a secondary antibody against human IgG Fc (clone HP6017). Cells were analyzed on an LSR II or Fortessa flow cytometer (BD Bioscience) and using FlowJo software (TreeStar, Ashland, OR, USA).

Ex vivo stimulation to assess T cell function

Cytokine production by T cells was assessed after *ex vivo* stimulation with M45 (HGIRNASFI), M38 (SSPPMFRV), B8R (TSYKFESV), SL8 (SIINFEKL) or gp100 (EGSRNQDWL) peptides (all synthesized by Genemed Synthesis, San Antonio, TX). To this end, $1 – 2 \times 10^6$ cells were incubated in T-cell media in a round bottom 96-well plate for 5 hours at 37° C in 5% CO_2. The final incubation volume was 100 μl and contained 1 μg/ml of the indicated peptide and 1 μg/ml brefeldin A (GolgiPlug, BD Biosciences), as well as fluorescently labeled antibody specific for CD107a. For stimulation of enriched $CD8^+$ T cells (Supplemental Fig. 3A), IFN-γ-treated M2-10B4s were used as antigen-presenting cells. M2-10B4s were plated at 100,000 cells/well in 12 well plates. After 4 hours, 2 ml of media with IFN-γ (Biolegend) at 100ng/ml was added. Treated M2-10B4s were used for $CD8^+$ T cell stimulation after 48 hours, a time point at which they expressed high levels of class I MHC and PD-L1 (not shown). Approximately 50,000 enriched $CD8^+$ T cells were added to each well and stimulated with peptides as above. In all cases, at the end of the stimulation period, cells were washed twice with ice-cold FACS buffer (PBS, 0.05% Sodium Azide, 1% FBS) and stained with antibodies specific for surface proteins followed by analyses of intracellular IFN-γ and TNF-α using the BD Cytofix/Cytoperm kit (BD Biosciences) and following the manufacturers instructions. Cells were analyzed by flow cytometry as above.

Adoptive transfers, *in vitro* T cell activation, and intravenous antibody injections

Adoptive transfers were performed as described previously [25]. The number of transferred cells and the timing of transfer and infection are stated in each figure legend. For the experiments in Fig. 6 and Suppl. Fig. 3A, OT-Is and Pmel-Is were co-transferred into mice one day before implantation of B16F0s. Recipients were co-infected with MCMV-SL8 and MCMV-gp100 5 days after tumor implantation to expand both OT-Is and Pmel-Is. For *in*

vitro activation, OT-Is were either taken from fresh or frozen naïve splenocytes (frozen in T cell media plus 10% DMSO) and enriched via magnetic negative CD8 selection as described above. Enriched cells were activated with anti-CD3/CD28 coated Dynabeads (ThermoFisher Scientific) following the manufacturer's protocol in T cell media containing 30 U/ml rIL-2 (Biolegend). Upon transfer, OT-Is were 90–100% alive (determined by Zombie Aqua™ Fixable Viability Kit [Biolegend]), 95–100% $CD44^{hi}$ (determined by anti-CD44 [clone IM7]), and had expanded 20–30 times.

Fluorescence Microscopy

Isolated tumors were frozen in OCT and sectioned using a cryostat. Sections were stained as previously described [26] with anti-CD31 (clone 390), anti-CD45.2 (clone 104) and DAPI (Prolong Gold antifade – Life Technologies), along with the anti-CD8α antibody injected IV prior to sacrifice to distinguish intra-vascular T cells. Images were generated with the LSM 510 Meta confocal laser scanning microscope (Carl Zeiss), the LSM image browser software (Carl Zeiss), and ImageJ (Fiji).

PCR for expression of full-length PD-1

Mice that had received both OT-Is and Pmel-Is (as described above) were used. When tumors were >100 mm^2, OT-Is and Pmel-Is were sorted from tumors with a FACS Aria (BD Bioscience) using the markers CD45.1 and Thy1.1 respectively (Supplemental Fig. 1E). RNA was extracted from sorted cells with the Arcturus PicoPure RNA isolation kit (Applied Biosystems) according to the manufacturer's instructions. cDNA was made using the High Capacity Reverse transcription kit from Applied Biosystems. PD-1 was amplified by nested PCR with primers designed to span from Exon 1 to Exon 5 as follows: outside primers (Forward: 5' GCA GGT ACC CTG GTC ATT CAC TTG G 3', Reverse: 5'ACA CAG GCG GTA GGG AGC TCT GGT 3') followed by amplification with inside primers (Forward: 5' AGC TGG CAA TCA GGG TGG CTT CTA G 3', Reverse: 5' ACA CTA GGG ACA GGT GCT GCT GAA GG 3'). The dominant PCR fragment corresponding to the size expected for full-length PD-1 was gel purified and sequenced to confirm the PCR fidelity. Sequenced products contained all 5 PD-1 exons.

Results

MCMV-gp100 infection induces TAA and virus-specific $CD8^+$ TIL

To study TAA-specific and virus-specific $CD8^+$ T cells in the same tumor, we used a recombinant MCMV expressing an altered gp100 epitope (MCMV-gp100) that drives expansion of gp100-specific T cells [24]. C57BL/6J mice ($Thy1.2^+$) received congenic ($Thy1.1^+$) Pmel-I transgenic T cells (specific for gp100) one day before B16F0s were implanted subcutaneously. Five days after tumor implantation, mice were infected with MCMV-gp100, which induced the expansion of gp100-specific Pmel-I T cells in the periphery and tumor, in contrast to wild-type MCMV (WT-MCMV, Fig. 1A). However, after either infection, MCMV-specific $CD8^+$ T cells were readily detected in tumors (Fig 1B and C) and at least 20% of the $CD8^+$ T cells in tumors were MCMV-specific (Fig. 1D and data not shown). Representative gating for this and subsequent experiments are shown in Supplementary Fig. 1. This phenomenon was not restricted to the transplanted B16F0

model, as MCMV-gp100 infection also drove MCMV-specific CD8$^+$ T cells into autochthonous tumors that arose in the Cre-inducible, BRAFV600E transgenic mouse model (Fig. 1E21]).

CD8$^+$ TIL are defined as being embedded in the tumor tissue. Using intravenous (IV) CD8α labeling to distinguish CD8$^+$ T cells that had migrated out of the vasculature [25, 27] we found that the vast majority of TAA and MCMV-specific CD8$^+$ T cells recovered with tumors were unlabeled and thus, within the tumor tissue (Fig. 1F). These data were confirmed histologically using congenically marked OT-I transgenic T cells that were driven by infection with MCMV expressing the SIINFEKL peptide from OVA (MCMV-SL8), a model in which OT-Is respond comparably to T cells driven by WT-MCMV infection [23]. In this model, B16F0s do not express OVA and therefore OT-Is can be considered virus-specific. Notably, GFP expression from the virus is undetectable *in vivo* by histological analysis (data not shown). However, most OT-I T cells were readily detected within the tumor tissue, with some OT-Is still associated with the tumor vasculature (CD8α IV$^+$, white arrow) (Fig. 1G), thus confirming the flow cytometry results. Together, these data show that virus-specific CD8$^+$ T cells can become TIL alongside TAA-specific TIL.

Activated CD8$^+$ T cells become TIL in the absence of viral replication or antigen

CMV protein has been found in multiple human tumors [28–31], can infect leukemia and melanoma *in vitro* [24, 32, 33] and we have seen MCMV DNA in B16F0 tumors from acutely and latently infected animals (data not shown). Thus, it is possible that MCMV-specific T cells entered tumors because the tumors were infected. To rule this out, we infected mice with a recombinant MCMV expressing the thymidine kinase gene from Herpes Simplex Virus (MCMV-TK), which enables inhibition of viral replication by the drug famcyclovir [34]. Tumor-bearing mice were infected in the foot-pad to localize the primary infection and treated or not with famcyclovir. This protocol prevents detection of viral DNA in the salivary gland of mice (not shown), normally a major target of MCMV infection, illustrating the ability of famcyclovir to limit viral spread. Regardless of famcyclovir treatment, MCMV-specific CD8$^+$ T cells became TIL in similar percentages (Fig. 2A and B). MCMV infects migratory monocytes and it is therefore possible that viral antigen was brought to the tumor in MCMV-infected monocytes in the absence of viral replication. To remove antigen from the system entirely, OT-I T cells were activated *in vitro* with antibodies targeting CD3 and CD28. Upon transfer into tumor-bearing mice, activated OT-Is also became TIL (Fig. 2C and D). Together, these data suggest that activation of CD8$^+$ T cells can promote entry into tumor tissue regardless of the presence of viral antigen.

MCMV-specific CD8$^+$ TIL are more functional than TAA-specific CD8$^+$ TIL, despite PD-1 expression

To explore the function of TAA-specific TIL, Pmel-I T cells (gp100-specific) were recovered from B16F0 tumors after infection with MCMV-gp100 and stimulated *ex vivo* to assess cytokine production and degranulation, as in Figure 1. As expected, TAA-specific Pmel-Is in the tumor were severely dysfunctional for cytokine production compared to Pmel-Is in the spleen, seven days after infection (Supplementary Fig. 2A), and when mice were sacrificed with tumors measuring >100 mm^2 (Fig. 3A). To measure the function of

MCMV-specific TIL in these same tumors, we quantified T cells by tetramer staining and compared these values to the number of cells that produced IFN-γ and TNF-α after stimulation with the same viral peptides (Supplementary Fig. 2B). By assessing the ratio of tetramer-staining to cytokine producing T cells, we can determine the proportion of functional, virus-specific T cells. In these analyses, a ratio of 1 indicates that the same number of T cells was identified by both tetramer staining and cytokine production after *ex vivo* stimulation. Strikingly, MCMV-specific T cells in the spleen and tumor were equally functional by this measure (Fig. 3B), indicating that T cell dysfunction within the tumor environment was restricted to TAA-specific TIL.

The preceding functional assays were performed with unsorted tumor homogenates. To test whether the tumor-milieu or the presence of tumor cells in the assay were skewing the results, OT-I T cells (virus-specific, CD45.1$^+$) and Pmel-I T cells (TAA-specific, Thy1.1$^+$) were co-transferred into B6 mice (CD45.2$^+$, Thy1.2$^+$), and both driven into B16F0 tumors by a mixed MCMV-SL8 and MCMV-gp100 infection (Supplementary Fig. 1E). CD8$^+$ T cells were isolated from the tumor with magnetic beads and stimulated with peptide using IFN-γ treated M2-10B4s as antigen presented cells. Although isolation from the tumor milieu improved the cytokine production by TAA-specific Pmel-I T cells as expected (Supplemental Figure 3A compared to Figure 3A), they were still less functional than Pmel-I T cells isolated from the spleens of the same animals. In contrast, virus-specific OT-Is from the tumor were equally functional to OT-Is isolated in the spleen, and substantially more functional than Pmel-Is isolated from the same tumors (Supplementary Fig. 3A). Thus, virus-specific tumor-infiltrating T cells remain functional within the tumor environment, in contrast to TAA-specific T cells from the same tumor.

The differences in function between TAA-specific and MCMV-specific T cells suggested that there may be differences in expression of immune inhibitory molecules such as PD-1 between the two TIL populations. Indeed, previous work has shown that MCMV-specific T cells in the spleens of non-tumor-bearing mice do not express PD-1 after the initial phases of MCMV infection [35]. Surprisingly, MCMV-specific T cells in the tumor expressed PD-1 at frequencies that were indistinguishable from Pmel-Is in the tumor (Fig. 3C), despite their markedly different functionality. To explore this more completely, OT-I T cells were driven into B16F0 tumors by MCMV-SL8 infection (Supplementary Fig. 3B). Seven days after infection, OT-Is in the tumor and blood expressed PD-1 (Fig 3D and E), as an expected result of recent clonal expansion. Interestingly, the mean fluorescence intensity of PD-1 expression was higher in the tumor than in the blood at this day 7 time point (Fig. 3E, $p = 0.038$). Even more strikingly, OT-Is in the tumor still expressed PD-1 14–16 days after infection with undiminished mean fluorescence intensity (Fig. 3D and 3E), in contrast to OT-I T cells in the blood, which had lost PD-1 expression by this time after infection. Notably, PD-1 expression was markedly higher on OT-Is embedded in the tumor tissue compared to cells in the tumor vasculature of the same tumor (Supplemental Fig. 3C). Despite this elevated and sustained PD-1 expression, these OT-I TIL remained fully functional for cytokine production both one and two weeks after infection (Fig. 3F), albeit with a slight reduction in degranulation (Supplementary Fig. 3D). Together, these data suggest that MCMV-specific CD8$^+$ TIL remain functional in the tumor environment, despite PD-1 expression, and that PD-1 expression induced during clonal expansion is maintained

on virus-specific CD8$^+$ TIL in contrast to cells found within the blood and the tumor vasculature.

Vaccinia-specific CD8$^+$ T cells become TIL and retain function, despite PD-1 expression

To determine whether these results were unique to MCMV infection, we used Vaccinia virus expressing OVA (VacV-OVA). As above, OT-Is were transferred one day before B16F0s were implanted, and mice were infected with VacV-OVA 5 days after tumor implantation. Both B8R-specific endogenous CD8$^+$ T cells (specific for VacV) and OT-Is expanded and migrated into tumor tissue (Fig. 4A and B) where they remained functional for cytokine production and degranulation (Fig. 4C, D and Supplementary Fig. 3D), despite expressing PD-1 within the tumor environment, as assessed by CD8α IV-staining (Fig. 4E, F). These data show that, like MCMV-specific T cells, VacV-specific CD8$^+$ T cells become TIL during acute viral infection and remain functional despite PD-1 expression.

Virus-specific CD8$^+$ T cells enter the tumor tissue during latent and cleared infections, retaining function

To this point, our data show that T cells activated in culture or responding to an acute viral infection, infiltrate tumor tissue. At these times, most virus-specific T cells are short-lived effector cells that have recently undergone clonal expansion [36, 37]. However, circulating T cell populations will also include resting memory T cells from previously encountered and cleared infections, as well as T cells participating in the control of persistent infections. VacV is cleared from B6 mice, allowing VacV-specific T cells to become resting memory T cells [38, 39]. To determine whether these resting memory T cells would infiltrate tumors, B16F0s were implanted into mice that had been infected with VacV 42–49 days previously, a time point at which all B8R-specific T cells in the blood were PD-1 negative and >50% had lost expression of the effector marker KLRG-1 (data not shown). Resting B8R-specific CD8$^+$ T cells still became TIL (Fig. 5A and B) and many of these TIL expressed low or intermediate levels of PD-1 within the tumor environment (Fig. 5C). Thus, resting memory virus-specific T cells that enter the tumor can also express PD-1. Interestingly, PD-1 expression on resting VacV-specific T cells that entered the tumor was low or intermediate and a substantial proportion of these cells lacked detectible PD-1 expression in the tumor environment. Thus, although PD-1 expression in the tumor may not depend on recent acute infection and clonal expansion, the PD-1 expression levels may correlate with recent antigen exposure.

Like all herpesviruses, MCMV induces a persistent/latent infection that requires continuous immune surveillance for life-long control [17, 18]. Everyone in the world is infected with multiple herpesviruses, making life-long immune surveillance common [16]. Most MCMV-specific T cells are driven into a state of terminal differentiation by this ongoing immune surveillance, although PD-1 is not expressed on these T cells at this stage of infection in mice or in HCMV-infected humans [35, 36, 40]. To determine whether MCMV-specific CD8$^+$ T cells would become TIL during persistent/latent MCMV infection, we implanted B16F0 tumors into mice infected with MCMV 8 to 12 weeks previously. Again, MCMV-specific CD8$^+$ T cells were present in tumors (Fig. 5D) and embedded in the tumor tissue (Fig. 5E) where they were fully functional for cytokine production (Fig. 5F). In this setting,

PD-1 could be detected on some MCMV-specific TIL that infiltrated tumors during the persistent phase of infection, although a large percentage of these cells lacked PD-1 (Fig. 6G). Similar data were seen with M45-specific T cells (data not shown), which represent a resting memory MCMV-specific population during the persistent/latent phase of infection [36, 41]. Together these data show that virus-specific $CD8^+$ T cells in circulation become TIL and remain functional regardless of whether an infection has been cleared or remains persistent. Moreover, these data suggest that PD-1 expression can be detected on virus-specific T cells that enter the tumor at any stage after activation, even when PD-1 expression has been lost on T cells in circulation. However, T cells that enter the tumor after acute infection and clonal expansion were more uniformly $PD\text{-}1^{high}$, compared to T cells that became TIL long after the acute infection had been resolved.

Virus-specific $CD8^+$ T cells express lower amounts of full length PD-1

Our data to this point showed that virus-specific TIL expressed PD-1 in the tumor environment, but remained functional. To directly compare PD-1 expression by virus-specific and TAA-specific T cells, we co-transferred ova-specific OT-I T cells and gp100-specific Pmel-I T cells, implanted tumors one day later, and infected the recipients with both MCMV-SL8 and MCMV-gp100 five days after that. TAA-specific Pmel-I T cells in the tumor uniformly expressed high levels of PD-1, while OT-I T cells recovered from the same tumors expressed significantly less PD-1 per cell (Fig. 6A and B). This result that was also evident with a second PD-1-binding antibody, clone 29F.1A12 (Fig. 6B), which blocks PD-L1 and PD-L2 binding to PD-1 ([42] and not shown). This reduced expression of PD-1 by virus-specific T cells correlated with an undetectable binding of recombinant, dimerized versions of the ligands PD-L1 (Fig. 6C) and PD-L2 (not shown), in contrast to Pmel-I T cells in the same tumors. Because splice variants of PD-1 have been described [43], the transcripts expressed by OT-Is and Pmel-Is isolated from tumors were amplified by RT-PCR. Primers were designed to span from the 1st to the 5th exon, mirroring the published strategy [43]. The major PCR product corresponded to the expected size for transcripts containing all 5 exons (Fig. 6D), a conclusion that was confirmed by sequence analysis (not shown). Together, these data suggest that both virus-specific and TAA-specific TILs expressed full-length and properly folded PD-1, but that reduced expression of PD-1 on virus-specific TIL reduced the interaction between PD-1 and its ligands PD-L1 and PD-L2.

PD-1 expression on virus-specific $CD8^+$ TIL is a marker of recent antigen stimulation, not a correlate of dysfunction

PD-1 expression is linked to recent or repeated antigen stimulation [9–13]. One major difference between TAA-specific TIL and virus-specific TIL is the availability of antigen in the tumor environment. To show that antigen in the tumor environment promotes high levels of PD-1 expression on TILs, we transferred congenic Pmel-Is into mice without tumors and expanded them with MCMV-gp100 infection (Supplementary Fig. 4A). Although PD-1 was expressed on Pmel-Is 7 days after infection as expected due to recent stimulation, these cells lost PD-1 expression by day 28 (Fig. 7A). On day 30 or 31, B16F0s were implanted. When tumors were 20–30 $mm^2$14–35 days after implantation, Pmel-Is had migrated into the tumors (Supplementary Fig. 4B) and uniformly expressed high levels of PD-1 (Fig. 7B). These data show that TAA-specific T cells lacking PD-1 robustly upregulated PD-1 upon

entry into tumors, unlike virus-specific T cells lacking PD-1 at the time of tumor entry (Fig. 5C and G). To test whether anti-viral TILs would also express high levels of PD-1 upon antigen encounter in tumors, B16F0s were implanted in mice infected for 30 days with wild-type MCMV, a time point at which MCMV-specific T cells in circulation lacked PD-1 (Fig. 7C). When tumors were 20 mm^2, they were directly injected with the MCMV-derived M38 peptide or DMSO as a negative control. One week later, M38-specific TIL uniformly expressed high levels of PD-1, in mice that received the M38 peptide. In contrast, M38-specific T cells in mice injected with DMSO only expressed low or intermediate levels of PD-1 and many cells were PD-1-negative (Fig. 7D), consistent with previous results (compare to Fig 5G). Irrespective of PD-1 expression, M38-specific T cells did not lose function as assessed by IFN-γ production after *ex vivo* stimulation (Fig. 7E), which is expected given the transient nature of antigen stimulation in this experiment. Collectively, these data show that the $CD8^+$ TIL population can reflect the specificity of the circulating T cell populations in an individual. Moreover, while antigen stimulation induces uniformly high levels of PD-1 expression, tumor infiltration promotes or sustains low or intermediate levels of PD-1 that do not correlate with cellular dysfunction.

Discussion

As tumor immunotherapy burgeons, prognostic and diagnostic TIL assays will become more common to assess treatment options and outcomes. Our data show that acute, cleared, and latent viral infections induce virus-specific $CD8^+$ TIL in melanoma tumors independent of viral replication or antigen, and that PD-1 expression was induced or sustained on virus-specific TILs in the absence of a deliberate introduction of antigen. Thus, these data suggest that the TIL status of an individual, at least in some tumors, will reflect their immune status, and that previously and recently activated T cells may “muddy” prognostic and diagnostic TIL analysis.

We considered the possibility that virus-specific $CD8^+$ T cells became TIL because the infection had spread to the B16F0 tumors. We have detected MCMV DNA within B16F0 tumors after acute infection as well as in latently infected mice (not shown). However, blocking MCMV replication at a distal site of infection (the footpad) had no impact on MCMV-specific TIL formation (Fig. 2A and B). In addition, *in vitro* activated $CD8^+$ T cells were able to enter tumors in the complete absence of virus (Fig. 2C and D). Therefore, viral infection of the tumor was not a requirement for T cell entry.

We also considered the possibility that T cell differentiation status would impact the formation or function of TIL. In the current study, we explored this functionally, by comparing virus-specific TIL formation after acute, persistent or cleared infections. Acute infections with MCMV and VacV produce large populations of short-lived effector T cells [36, 37], while MCMV persistence sustains large numbers of effector-differentiated cells and very few memory-phenotype T cells [36, 41, 44]. In contrast, clearance of VacV allows cells to develop into resting memory cells [37]. In all cases, virus-specific TIL developed, suggesting that T cell differentiation was not the major determinant of TIL formation. Notably, naïve $CD8^+$ T cells have been shown to enter B16 tumors and become TIL as well ([19] and our own unpublished data), suggesting that even T cell activation is not a pre-

requisite for entry into tumors. Collectively, these data suggest that naïve, activated, or resting memory CD8$^+$ T cells have access to tumors and become part of the normal TIL population in an antigen independent manner (summarized in Fig. 8A and B).

The presence of low and intermediate levels of PD-1 on virus-specific TIL was surprising. In many chronic infections and in tumor-bearing individuals, antigen-specific CD8$^+$ T cells become highly dysfunctional, correlating with PD-1 expression and repeated antigen exposure [9–12, 45, 46]. However, virus-specific T cells retained the ability to secrete cytokines in the tumor despite expression of the full-length PD-1 transcript (Fig. 6). Tumor-localized T cells retained PD-1 expression even while cells in the circulation lost PD-1 (Fig. 3D and E and summarized in Fig. 8 A and B). Moreover, increased PD-1 expression could be detected on virus-specific T cells that migrated into tumors long after the primary infection and, in the case of VacV infection, clearance of the virus. Interestingly, cells that had recently undergone clonal expansion retained relatively higher levels of PD-1 compared to cells that migrated into the tumor long after the primary infection (Fig. 3 to 6). Importantly, antigen encounter within the tumor environment induced robust and uniform PD-1 expression on both TAA-specific T cells as well as virus-specific T cells, as expected (Fig. 7). These data suggest that virus-specific TIL were not encountering antigen in the tumor environment unless it was deliberately injected, and that our results cannot be explained by viral infection of the tumor or T cells that are cross-reactive to both viral and tumor antigens. As summarized in Fig. 8, we interpret these data to suggest that virus-specific T cells in the tumor rarely interact with antigen (or PD-1 ligands) and that PD-1 expression on TILs is supported by the tumor environment independently of antigen exposure. Notably, certain cytokines are capable of inducing PD-1 expression in stimulated T cells [47]. Thus, our data suggest that the critical difference between virus-specific and TAA-specific TIL is the absence of constitutive antigen presentation by cells in the tumor, rather than PD-1 expression *per se* (Fig. 8B and C).

Although our data show that virus-specific TIL expressed cytokines normally, future work will be needed to determine whether the intermediate expression of PD-1 has any impact on proximal signaling events through the TCR or overall T cell function. Notably, virus-specific TIL displayed reduced CD107a exposure, a marker of degranulation, after peptide stimulation *ex vivo* (Supplemental Fig. 3D). This decreased degranulation fits with recent studies of PD-1$^+$ CD8$^+$ T cells in various tissues during chronic infections, which were all deficient in their ability to degranulate and kill despite differences in ability to produce cytokines [48]. Thus, although virus-specific TIL are clearly not exhausted, they may not be fully functional in the tumor environment and future studies will be required to explore this possibility.

If circulating naïve and activated T cells become TIL regularly, this could skew prognostic and diagnostic TIL assays, as some of the TIL would be irrelevant for the prognosis or the success of immunotherapy. Large numbers of PD-1$^+$ CD8$^+$ TIL that are specific for a virus, but not the tumor, might explain the failure of PD-1/PD-L1 blocking therapies in some patients [14, 49]. For these reasons, it is crucial to know how common this phenomenon is in other cancer models, and in a variety of human cancers, and perhaps develop tools that can exclude virus-specific TIL from diagnostic or prognostic assays. Our data suggest that PD-1

levels on $CD8^+$ TIL may be a better correlate of both TIL function and recent antigen exposure, even without knowing the specificity of the TIL populations. Thus, diagnostic assays designed to define the levels of PD-1 expression on TILs may provide valuable insights.

To our knowledge, this study is the first to preform comparative analyses of TAA-specific and virus-specific TIL in melanoma. Our data show that the TIL population in a tumor may be far more complex than previously believed and that an individual's immune status may shape their TIL populations.

Supplementary Material

Refer to Web version on PubMed Central for supplementary material.

Acknowledgments

Grant Support: This work was supported by grants from the NIH (RO3 CA174979 and RO1 AI106810), and the American Cancer Society (ACS-IRG-08-060-04 and RSG-15-184-01) awarded to C.M.S.

References

1. Hadrup S, Donia M, Thor Straten P. Effector CD4 and CD8 T cells and their role in the tumor microenvironment. Cancer Microenviron. 2013; 6(2):123–133. [PubMed: 23242673]
2. Gooden MJ, de Bock GH, Leffers N, Daemen T, Nijman HW. The prognostic influence of tumour-infiltrating lymphocytes in cancer: a systematic review with meta-analysis. Br J Cancer. 2011; 105(1):93–103. [PubMed: 21629244]
3. Restifo NP, Dudley ME, Rosenberg SA. Adoptive immunotherapy for cancer: harnessing the T cell response. Nat Rev Immunol. 2012; 12(4):269–281. [PubMed: 22437939]
4. Hailemichael Y, Overwijk WW. Cancer vaccines: Trafficking of tumor-specific T cells to tumor after therapeutic vaccination. Int J Biochem Cell Biol. 2014; 53:46–50. [PubMed: 24796845]
5. Rosenberg SA, Restifo NP. Adoptive cell transfer as personalized immunotherapy for human cancer. Science. 2015; 348(6230):62–68. [PubMed: 25838374]
6. Manzo T, Heslop HE, Rooney CM. Antigen-specific T cell therapies for cancer. Hum Mol Genet. 2015; 24(R1):R67–73. [PubMed: 26160910]
7. Schuessler A, Walker DG, Khanna R. Cytomegalovirus as a novel target for immunotherapy of glioblastoma multiforme. Front Oncol. 2014; 4(275):1–5. [PubMed: 24478982]
8. Rosenberg SA, Yang JC, Sherry RM, Kammula US, Hughes MS, Phan GQ, Citrin DE, Restifo NP, Robbins PF, Wunderlich JR, Morton KE, Laurencot CM, Steinberg SM, White DE, Dudley ME. Durable complete responses in heavily pretreated patients with metastatic melanoma using T-cell transfer immunotherapy. Clin Cancer Res. 2011; 17(13):4550–4557. [PubMed: 21498393]
9. Baitsch L, Baumgaertner P, Devevre E, Raghav SK, Legat A, Barba L, Wieckowski S, Bouzourene H, Deplancke B, Romero P, Rufer N, Speiser DE. Exhaustion of tumor-specific CD8(+) T cells in metastases from melanoma patients. J Clin Invest. 2011; 121(6):2350–2360. [PubMed: 21555851]
10. Sakuishi K, Apetoh L, Sullivan JM, Blazar BR, Kuchroo VK, Anderson AC. Targeting Tim-3 and PD-1 pathways to reverse T cell exhaustion and restore anti-tumor immunity. J Exp Med. 2010; 207(10):2187–2194. [PubMed: 20819927]
11. Fourcade J, Sun Z, Benallaoua M, Guillaume P, Luescher IF, Sander C, Kirkwood JM, Kuchroo V, Zarour HM. Upregulation of Tim-3 and PD-1 expression is associated with tumor antigen-specific CD8+ T cell dysfunction in melanoma patients. J Exp Med. 2010; 207(10):2175–2186. [PubMed: 20819923]

12. Ahmadzadeh M, Johnson LA, Heemsterk B, Wunderlich JR, Dudley ME, White DE, Rosenberg SA. Tumor antigen–specific CD8 T cells infiltrating the tumor express high levels of PD-1 and are functionally impaired. Blood. 2009; 114(8):1537–1544. [PubMed: 19423728]
13. Wherry EJ. T cell exhaustion. Nature Immunology. 2011; 131(6):492–499.
14. Chen L, Han X. Anti-PD-1/PD-L1 therapy of human cancer: past, present, and future. J Clin Invest. 2015; 125(9):3384–3391. [PubMed: 26325035]
15. Gros A, Robbins PF, Yao X, Li YF, Turcotte S, Tran E, Wunderlich JR, Mixon A, Farid S, Dudley ME, Hanada K, Almeida JR, Darko S, Douek DC, Yang JC, Rosenberg SA. PD-1 identifies the patient-specific CD8(+) tumor-reactive repertoire infiltrating human tumors. J Clin Invest. 2014; 124(5):2246–2259. [PubMed: 24667641]
16. Virgin HW, Wherry EJ, Ahmed R. Redefining chronic viral infection. Cell. 2009; 138(1):30–50. [PubMed: 19596234]
17. Simon CO, Holtappels R, Tervo HM, Bohm V, Daubner T, Oehrlein-Karpi SA, Kuhnapfel B, Renzaho A, Strand D, Podlech J, Reddehase MJ, Grzimek NK. CD8 T cells control cytomegalovirus latency by epitope-specific sensing of transcriptional reactivation. J Virol. 2006; 80(21):10436–10456. [PubMed: 16928768]
18. Polić B, Hengelm H, Krmpotic A, Trgovcich J, Pavić I, Lučin P, Koszinowski UH. Hierarchical and Redundant Lymphocyte Subset Control Precludes Cytomegalovirus Replication during Latent Infection. J Exp Med. 1998; 188(6):1047–1054. [PubMed: 9743523]
19. Thompson ED, Enriquez HL, Fu YX, Engelhard VH. Tumor masses support naive T cell infiltration, activation, and differentiation into effectors. J Exp Med. 2010; 207(8):1791–1804. [PubMed: 20660615]
20. Quinn M, Erkes DA, Snyder CM. Cytomegalovirus and immunotherapy: opportunistic pathogen, novel target for cancer and a promising vaccine vector. Immunotherapy. 2016; 8(2):211–221. [PubMed: 26786895]
21. Dankort D, Curley DP, Cartlidge RA, Nelson B, Karnezis AN, Damsky WE Jr, You MJ, DePinho RA, McMahon M, Bosenberg M. Braf(V600E) cooperates with Pten loss to induce metastatic melanoma. Nat Genet. 2009; 41(5):544–552. [PubMed: 19282848]
22. Zurbach KA, Moghbeli T, Snyder CM. Resolving the titer of murine cytomegalovirus by plaque assay using the M2-10B4 cell line and a low viscosity overlay. Virol J. 2014; 11(71):1–9. [PubMed: 24393133]
23. Turula H, Smith CJ, Grey F, Zurbach KA, Snyder CM. Competition between T cells maintains clonal dominance during memory inflation induced by MCMV. Eur J Immunol. 2013; 43(5):1252–1263. [PubMed: 23404526]
24. Erkes DA, Xu G, Daskalakis C, Zurbach KA, Wilski N, Moghbeli T, Hill AB, Snyder CM. Intratumoral infection with murine cytomegalovirus synergizes with PD-L1 blockade to clear melanoma lesions and induce long-term immunity. Mol Ther. 2016; 24(8):1–12.. [PubMed: 26854182]
25. Smith CJ, Caldeira-Dantas S, Turula H, Snyder CM. Murine CMV Infection Induces the Continuous Production of Mucosal Resident T Cells. Cell Rep. 2015; 13(6):1137–1148. [PubMed: 26526996]
26. Smith CJ, Turula H, Snyder CM. Systemic hematogenous maintenance of memory inflation by MCMV infection. PLoS Pathog. 2014; 10(7):e1004233. [PubMed: 24992722]
27. Anderson KG, Mayer-Barber K, Sung H, Beura L, James BR, Taylor JJ, Qunaj L, Griffith TS, Vezys V, Barber DL, Masopust D. Intravascular staining for discrimination of vascular and tissue leukocytes. Nat Protoc. 2014; 9(1):209–222. [PubMed: 24385150]
28. Charles, S Cobbs, Minu Samanta, LH., Yancey Gillespie, G., Suman Bharara, King, Peter H., Burt Nabors, L., Glenn Cobbs, C., Britt, William J. Human Cytomegalovirus Infection and Expression in Human Malignant Glioma. Cancer Research. 2002; 62(12):3347–3350. [PubMed: 12067971]
29. Harkins L, Volk AL, Samanta M, Mikolaenko I, Britt WJ, Bland KI, Cobbs CS. Specific localisation of human cytomegalovirus nucleic acids and proteins in human colorectal cancer. The Lancet. 2002; 360(9345):1557–1563.

30. Harkins LE, Matlaf LA, Soroceanu L, Klemm K, Britt WJ, Wang W, Bland KI, Cobbs CS. Detection of human cytomegalovirus in normal and neoplastic breast epithelium. Herpesviridae. 2010; 1(1):1–8. [PubMed: 21429241]
31. Samanta M, Harkins L, Klemm K, Britt WJ, Cobbs CS. High prevalence of human cytomegalovirus in prostatic intraepithelial neoplasia and prostatic carcinoma. J Urol. 2003; 170(3):998–1002. [PubMed: 12913758]
32. Koldehoff M, Lindemann M, Opalka B, Bauer S, Ross RS, Elmaagacli AH. Cytomegalovirus induces apoptosis in acute leukemia cells as a virus-versus-leukemia function. Leuk Lymphoma. 2015:1–9.
33. Wu QH, Trymbulak W, Tatake RJ, Forman SJ, Zeff RA, Shanley JD. Replication of human cytomegalovirus in cells deficient in p2-microglobulin gene expression. Journal of General Virology. 1994; 75:2755–2759. [PubMed: 7931162]
34. Snyder CM, Cho KS, Bonnett EL, Allan JE, Hill AB. Sustained CD8+ T cell memory inflation after infection with a single-cycle cytomegalovirus. PLoS Pathog. 2011; 7(10):1–14.
35. Snyder CM, Loewendorf A, Bonnett EL, Croft M, Benedict CA, Hill AB. CD4+ T cell help has an epitope-dependent impact on CD8+ T cell memory inflation during murine cytomegalovirus infection. J Immunol. 2009; 183(6):3932–3941. [PubMed: 19692644]
36. Quinn M, Turula H, Tandon M, Deslouches B, Moghbeli T, Snyder CM. Memory T cells specific for murine cytomegalovirus re-emerge after multiple challenges and recapitulate immunity in various adoptive transfer scenarios. J Immunol. 2015; 194(4):1726–1736. [PubMed: 25595792]
37. Amoah S, Yammani RD, Grayson JM, Alexander-Miller MA. Changes in functional but not structural avidity during differentiation of CD8+ effector cells in vivo after virus infection. J Immunol. 2012; 189(2):638–645. [PubMed: 22706075]
38. Laouar A, Manocha M, Haridas V, Manjunath N. Concurrent generation of effector and central memory CD8 T cells during vaccinia virus infection. PLoS One. 2008; 3(12):1–8.
39. Xu R, Johnson AJ, Liggitt D, Bevan MJ. Cellular and Humoral Immunity against Vaccinia Virus Infection of Mice. The Journal of Immunology. 2004; 172(10):6265–6271. [PubMed: 15128815]
40. Hertoghs KM, Moerland PD, van Stijn A, Remmerswaal EB, Yong SL, van de Berg PJ, van Ham SM, Baas F, ten Berge IJ, van Lier RA. Molecular profiling of cytomegalovirus-induced human CD8+ T cell differentiation. J Clin Invest. 2010; 120(11):4077–4090. [PubMed: 20921622]
41. Snyder CM, Cho KS, Bonnett EL, van Dommelen S, Shellam GR, Hill AB. Memory inflation during chronic viral infection is maintained by continuous production of short-lived, functional T cells. Immunity. 2008; 29(4):650–659. [PubMed: 18957267]
42. Liang SC, Latchman YE, Buhlmann JE, Tomczak MF, Horwitz BH, Freeman GJ, Sharpe AH. Regulation of PD-1, PD-L1, and PD-L2 expression during normal and autoimmune responses. Eur J Immunol. 2003; 33(10):2706–2716. [PubMed: 14515254]
43. Nielsen C, Ohm-Laursen L, Barington T, Husby S, Lillevang ST. Alternative splice variants of the human PD-1 gene. Cell Immunol. 2005; 235(2):109–116. [PubMed: 16171790]
44. Sierro S, Rothkopf R, Klenerman P. Evolution of diverse antiviral CD8+ T cell populations after murine cytomegalovirus infection. Eur J Immunol. 2005; 35(4):1113–1123. [PubMed: 15756645]
45. Yi JS, Cox MA, Zajac AJ. T-cell exhaustion: characteristics, causes and conversion. Immunology. 2010; 129(4):474–481. [PubMed: 20201977]
46. Barber DL, Wherry EJ, Masopust D, Zhu B, Allison JP, Sharpe AH, Freeman GJ, Ahmed R. Restoring function in exhausted CD8 T cells during chronic viral infection. Nature. 2006; 439(7077):682–687. [PubMed: 16382236]
47. Austin JW, Lu P, Majumder P, Ahmed R, Boss JM. STAT3, STAT4, NFATc1, and CTCF Regulate PD-1 through Multiple Novel Regulatory Regions in Murine T Cells. J Immunol. 2014; 192(10): 4876–4886. [PubMed: 24711622]
48. Blackburn SD, Crawford A, Shin H, Polley A, Freeman GJ, Wherry EJ. Tissue-specific differences in PD-1 and PD-L1 expression during chronic viral infection: implications for CD8 T-cell exhaustion. J Virol. 2010; 84(4):2078–2089. [PubMed: 19955307]
49. Zhang Y, Kang S, Shen J, He J, Jiang L, Wang W, Guo Z, Peng G, Chen G, He J, Liang W. Prognostic significance of programmed cell death 1 (PD-1) or PD-1 ligand 1 (PD-L1) Expression in epithelial-originated cancer: a meta-analysis. Medicine (Baltimore). 2015; 94(6):1–10.

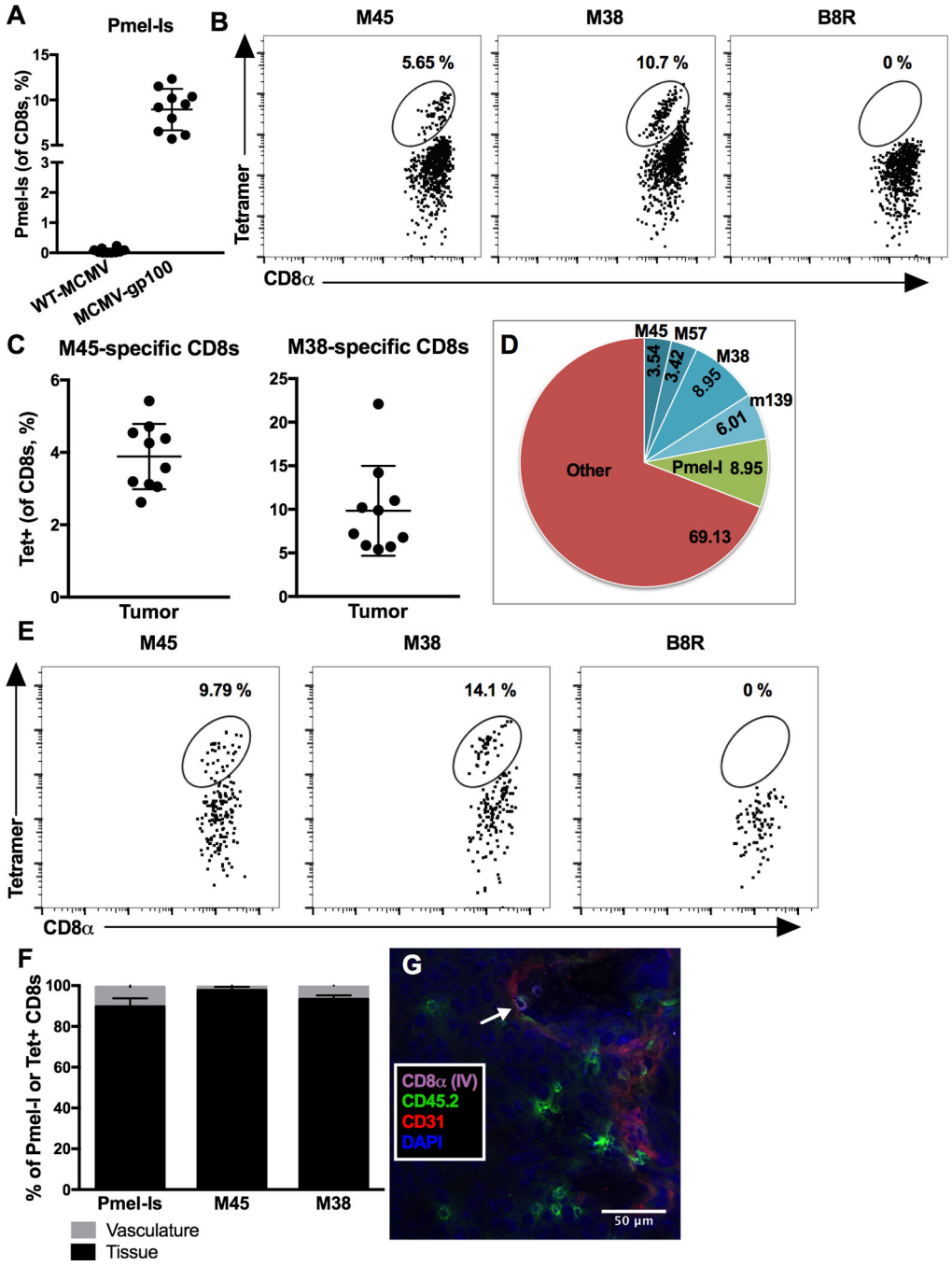

Figure 1. MCMV-gp100 infection results in migration of virus and TAA-specific CD8$^+$ T cells into melanoma tumors

A–D) Animals received 5 × 10^4 Pmel-Is on day -1 (D-1), 1 × 10^5 B16F0s on D0, and were infected with WT-MCMV (n=10) or MCMV-gp100 IP/ID (n=10) on D5. Mice were sacrificed for analyses when tumors were > 100mm^2, 11–33 days post infection. Shown is (A) the percentage of Pmel-I CD8$^+$ T cells (Thy1.1+) in the tumor, (B) representative FACS plots of MCMV-specific (M45 and M38) CD8$^+$ T cells in tumors, (C) the percentage of MCMV-specific CD8$^+$ T cells in individual mice, and (D) the average size of antigen-specific T cell populations in tumors from MCMV-gp100 infected mice. The data is

combined from 3 independent experiments, and A and C depict the mean +/− standard deviation (SD). The B8R-loaded tetramer shown in B was used as a negative control to establish the gates. E) Representative (n=5, 2 experiments) FACS plots of MCMV-specific $CD8^+$ T cells in autochthonous tumors from BRAFV600E transgenic mice at sacrifice. Mice were infected with MCMV-gp100 IP once a tumor was palpable. F) Mice received intravenous (IV) anti-CD8α to distinguish vascular and tissue-localized T cells. Shown is the percentage of IV-labeled or unlabeled Pmel-I, M45- and M38-specific CD8s in tumors from 4 mice from Fig. 1A–D. G) Mice received 10^3 OT-Is on D-1, B16F0s on D0, and MCMV-GFP-SL8 [23] on D5. The representative (n=4) immunoflouresence image shows OT-Is labeled with anti-CD45.2 (green) +/− the IV-delivered anti-CD8α antibody (purple) on D12. The white arrow points to a double-labeled OT-I. Endothelial cells were identified by CD31 staining (red).

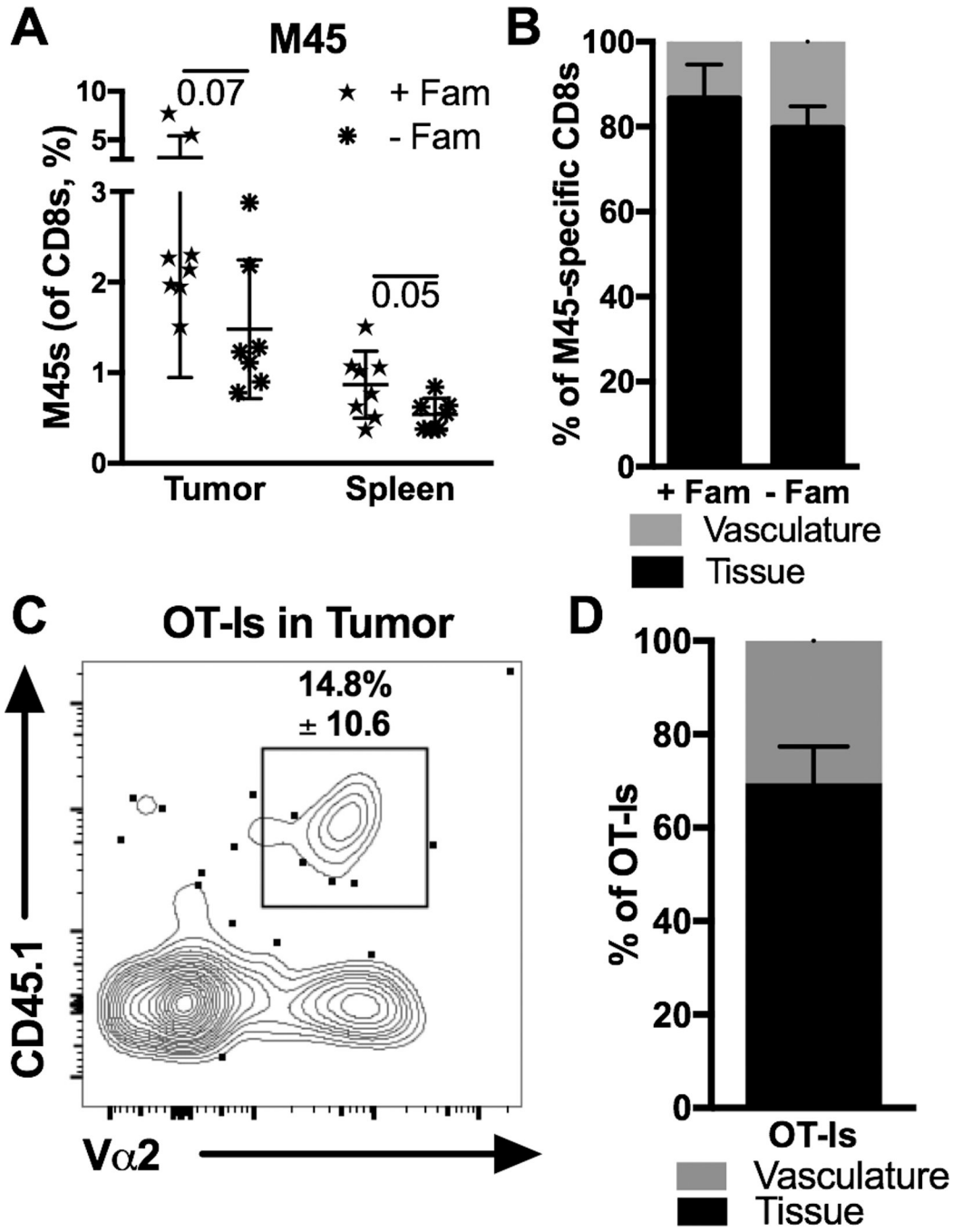

Figure 2. Activated CD8$^+$ TIL form in the absence of viral replication and antigen

A–B) Mice treated with famcyclovir (+Fam, n=8) or not (−Fam, n=7) as previously described [34] were implanted with B16F0s on D0, infected with MCMV-TK [34] on D5 via the footpad, and sacrificed on D19 for analyses. Shown is (A) the frequency of M45-specific CD8$^+$ T cells in the tumor and spleen and (B) the percentage of tetramer-binding cells in the tumor that were IV labeled or unlabeled. Significance in A was assessed by an unpaired t-test. C–D) *In vitro* activated OT-Is (3×10^6) were transferred into uninfected mice on D7 after B16F0 implantation. Shown is (C) a representative FACS plot of OT-Is (CD45.1$^+$,

Vα2^{+}) recovered from the tumor and (D) the percent of OT-Is that were labeled or not by IV CD8α staining, two days post transfer (n=4, 2 experiments). All data is represented as mean +/− SD.

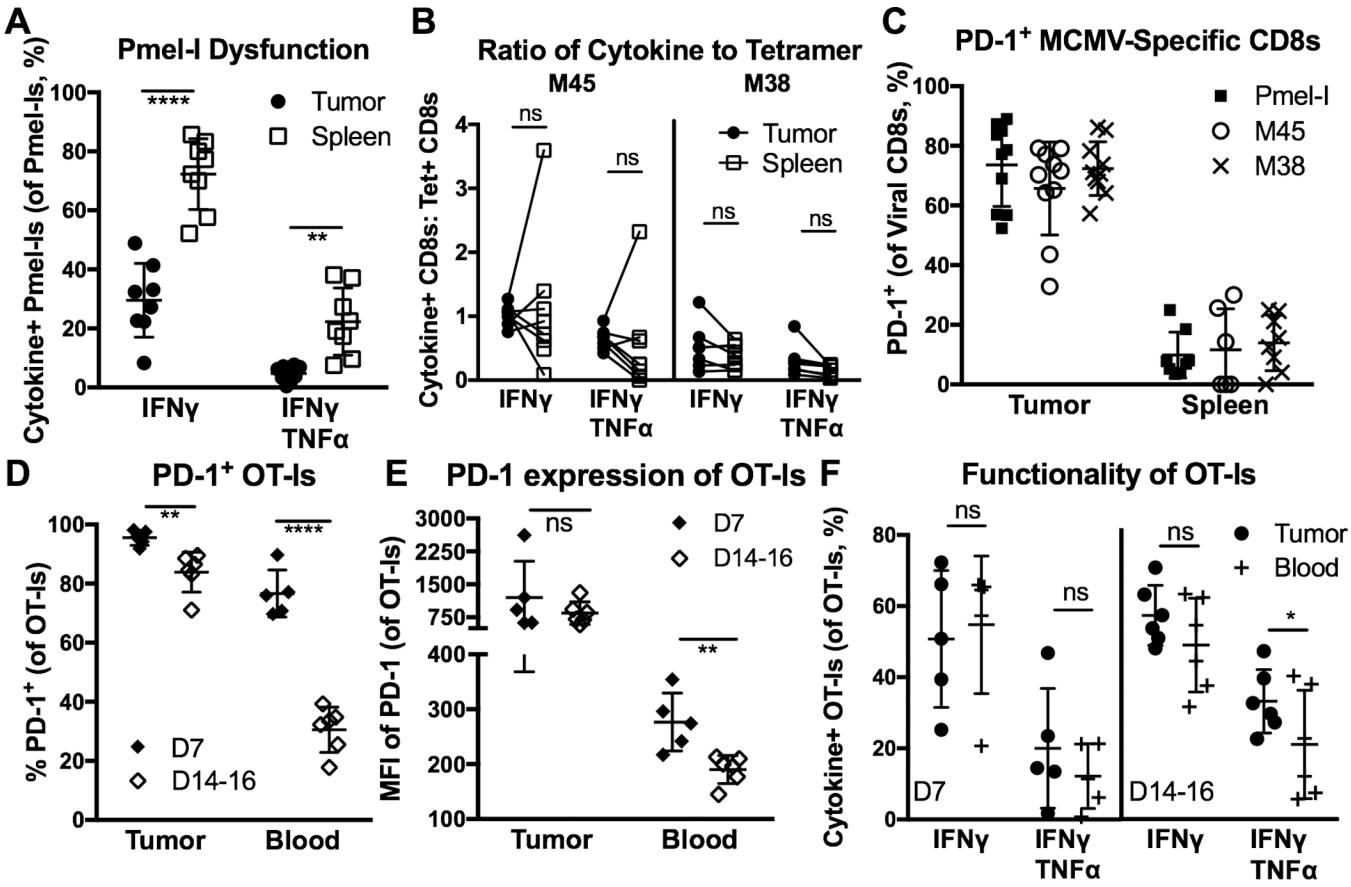

Figure 3. MCMV-specific CD8$^+$ T cells retain function in tumors despite high PD-1 expression

A–C) Animals were setup as in Fig. 1A, with MCMV-gp100 IP infection. Shown is (A) the percent of Pmel-Is that produced cytokines after *ex vivo* stimulation with gp100 peptide, (B) the functionality of MCMV-specific T cells in the tumor and spleen as assessed by the ratio of tetramer staining to cytokine production after *ex vivo* stimulation with peptide, and (C) the percent of Pmel-Is or MCMV-specific CD8s that were PD-1$^+$ at sacrifice. D–F) Animals received 10^3 OT-Is on D-1 and B16F0s on D0. Tumor-bearing mice were infected with MCMV-GFP-SL8 IP on D5, and sacrificed on D7 (n=5) or D14–16 (n=6) post-infection (P.I.). Shown is (D) the percent of OT-Is that were PD-1$^+$ 7 or 14 days P.I., (E) the PD-1 mean fluorescence intensity (MFI) on OT-Is in the tumors and blood of animals D7 or D14 after MCMV-SL8 infection, and (F) the percent of OT-Is recovered from the tumor or blood that produced cytokines after *ex vivo* stimulation. All data is represented as the mean +/− SD. Significance was assessed by paired (A, B, D) or unpaired (E) t-tests, $p < 0.05$ = *, $p < 0.01$ = **, $p < 0.0001$ = ****.

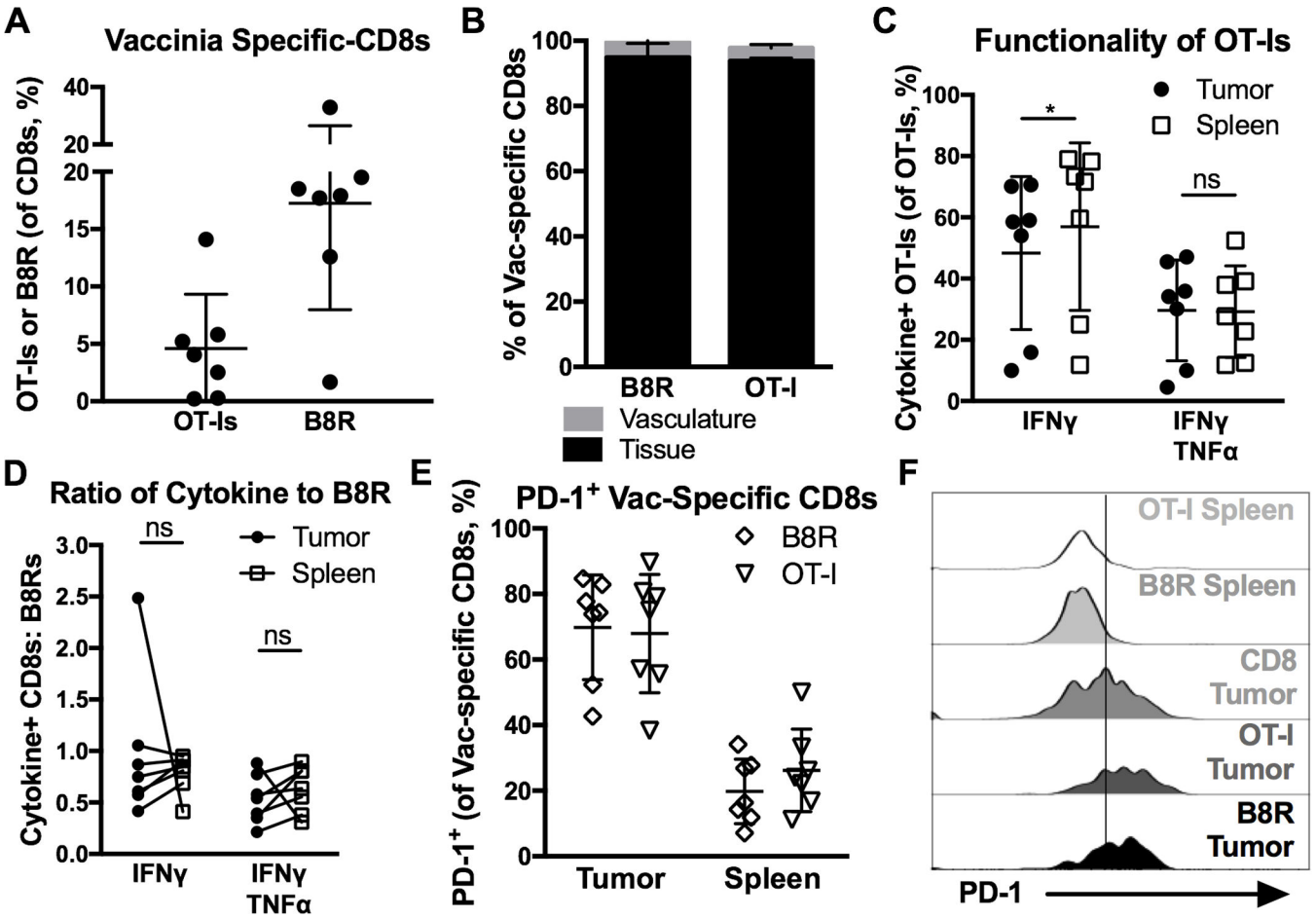

Figure 4. Vaccinia-specific CD8$^+$ T cells become TIL after acute infection and retain function despite PD-1 expression

Animals received 10^3 OT-Is on D-1, B16F0s on D0, were infected with VacV-OVA on D5, and sacrificed on D19 (n=7, 2 independent experiments) for tumor and spleen analysis. Shown is (A) the percent of Vaccinia-driven (OT-Is and B8R-specific) CD8$^+$ T cells in the tumor, (B) the percentage of CD8α IV positive and negative Vaccinia-driven CD8$^+$ T cells (n=4), (C) the percent of OT-Is that produced cytokine after *ex vivo* stimulation with peptide, (D) the functionality of VacV-driven T cells assessed as in Fig. 3B. E–F) Shown is the percent of cells that were PD-1$^+$ (E), and the MFI of PD-1 expression (F) on total and Vaccinia-specific CD8$^+$ T cells that were in the spleen (including CD8α IV positive and negative), and in the tumor tissue (only CD8α IV negative, n=7). All data is represented as the mean +/− SD. Significance in C and D was assessed by paired t-tests, $p < 0.05$ = *.

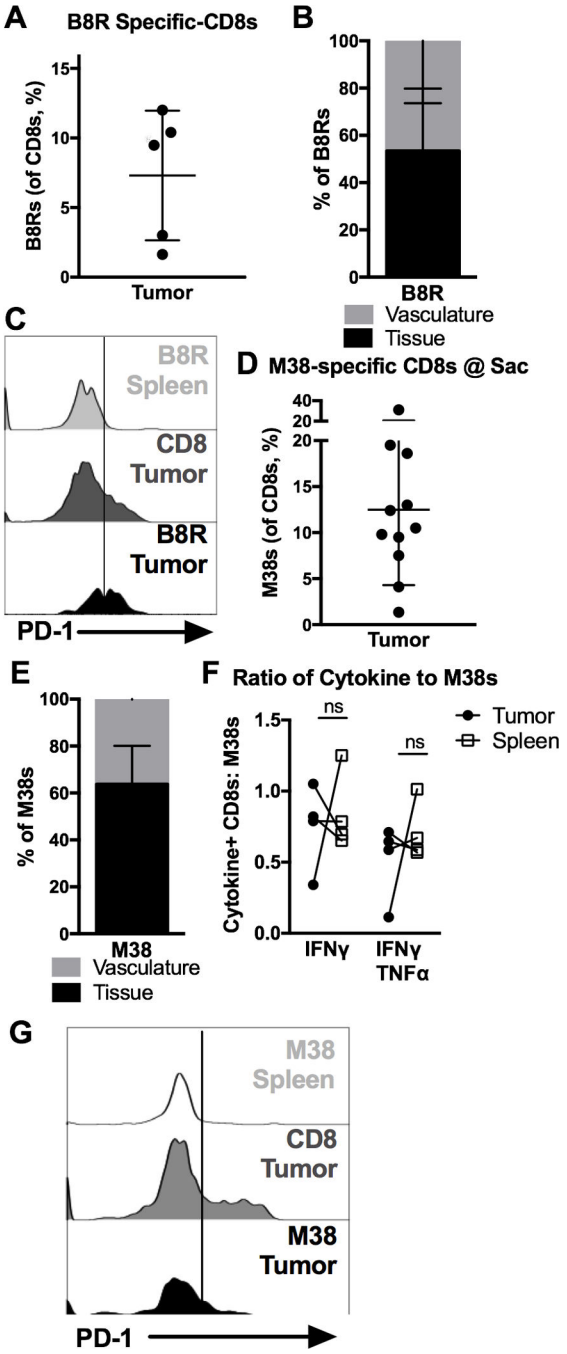

Figure 5. Virus-specific CD8s enter tumors, retain function, but express less PD-1 after cleared infections or during latent infections

A–C) Mice received B16F0s 42–49 days after VacV-OVA infection (n=5, 2 experiments) and were sacrificed 14 days later for tumor and spleen analysis. Shown is (A) the percent of B8R-specific $CD8^+$ T cells, (B) the percent of B8R-specific T cells in the tumor that were labeled by IV CD8α staining (n=4), and (C) the representative MFI of PD-1 on total and Vaccinia-specific $CD8^+$ T cells that were in the spleen (including both CD8α IV positive and negative), and in the tumor tissue (only CD8α IV negative, n=4). D-G) Mice received B16F0s >12 weeks after infection with MCMV strain K181 (n=11, 3 experiments) and were

sacrificed 21 days later, or for one mouse on day 17 when the tumor reached 100 mm^2. Shown is (D) the percent of MCMV-specific CD8s, (E) the proportion of MCMV-specific T cells in the tumor that were labeled by IV CD8α staining, (F) the functionality of MCMV-specific T cells, assessed as in Fig. 3B (n=4, representative of the whole), and (G) the MFI of PD-1 on total and MCMV-specific $CD8^+$ T cells that were in the spleen (including both CD8α IV positive and negative), and in the tumor tissue (only CD8α IV negative, n=7) All data is represented as the mean +/− SD and the significance (F) was assessed by paired t-tests, $p < 0.05$ = *.

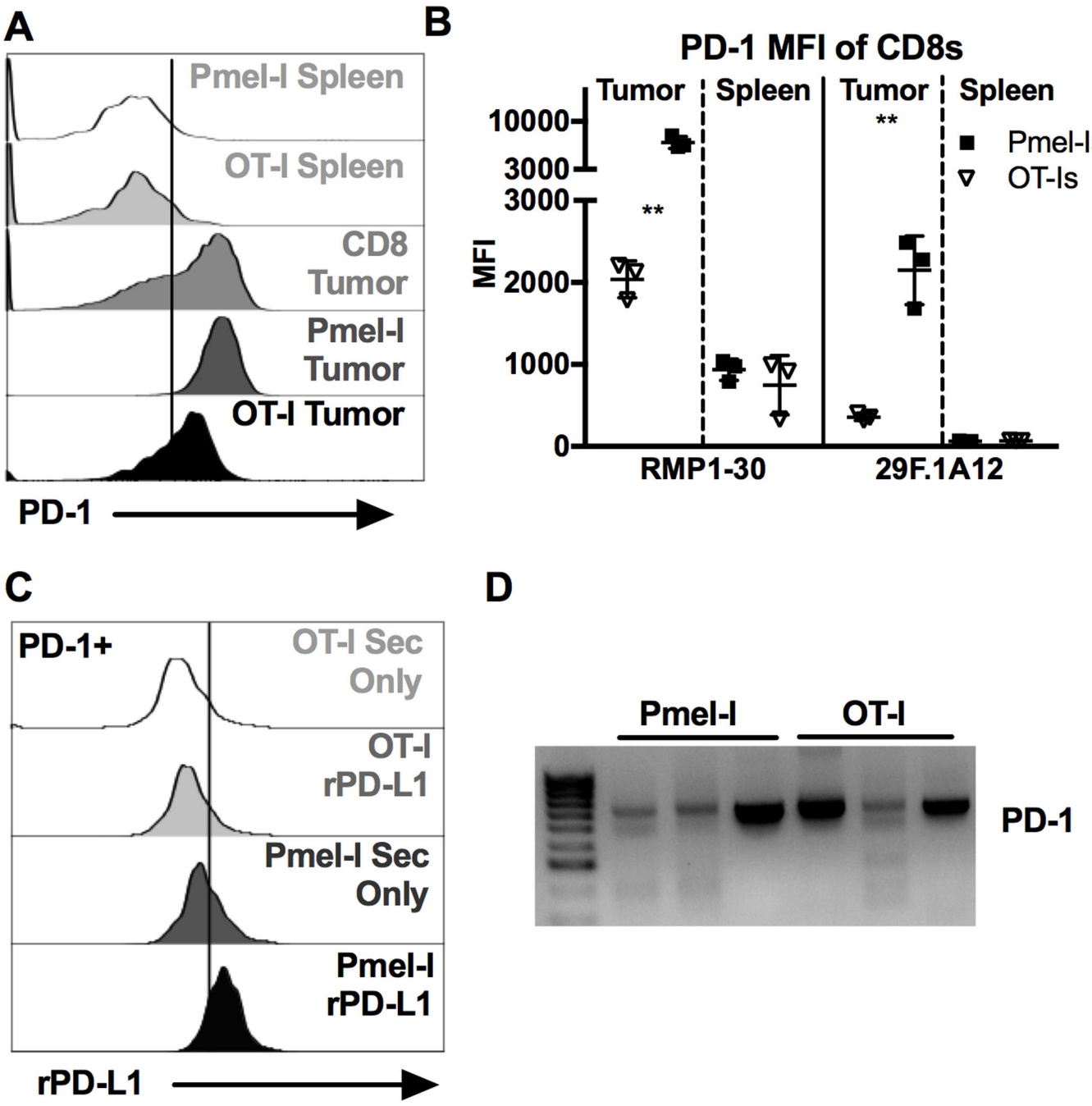

Figure 6. Virus-specific CD8$^+$ TIL express lower amounts of full length PD-1 than tumor-specific CD8$^+$ TIL, altering PD-L1 binding

500 OT-Is and 5000 Pmel-Is were co-transferred on D-1 and 1 × 10^5 B16F0s were given on D0. Tumor bearing animals were infected with 2 × 10^5 pfu of each MCMV-GFP-SL8 and MCMV-GP100 IP on D5. Mice were sacrificed when the tumor reached 100mm^2. Shown is (A) representative staining of PD-1 using clone RMP1–30 and (B) average MFI of PD-1 staining using clone RMP1–30 or clone 29F.1A12 for the indicated CD8$^+$ populations recovered from the same tumors (n=3). FACS plots of CD8$^+$ T cells in the spleen include both CD8α IV positive and negative cells while T cells in the tumor tissue include only the

CD8α IV negative subset. Significance in (B) was assessed by paired t-tests, $p < 0.01$ = **. C) Representative binding of recombinant PD-L1 to PD-1^+ virus-specific (OT-Is) and TAA-specific (Pmel-Is) recovered from the same tumor (n=4). D) PCR products of PD-1 (Exon 1 through 5) from cDNA derived from sorted virus-specific (OT-Is) and TAA-specific (Pmel-Is) $CD8^+$ TIL (n=3).

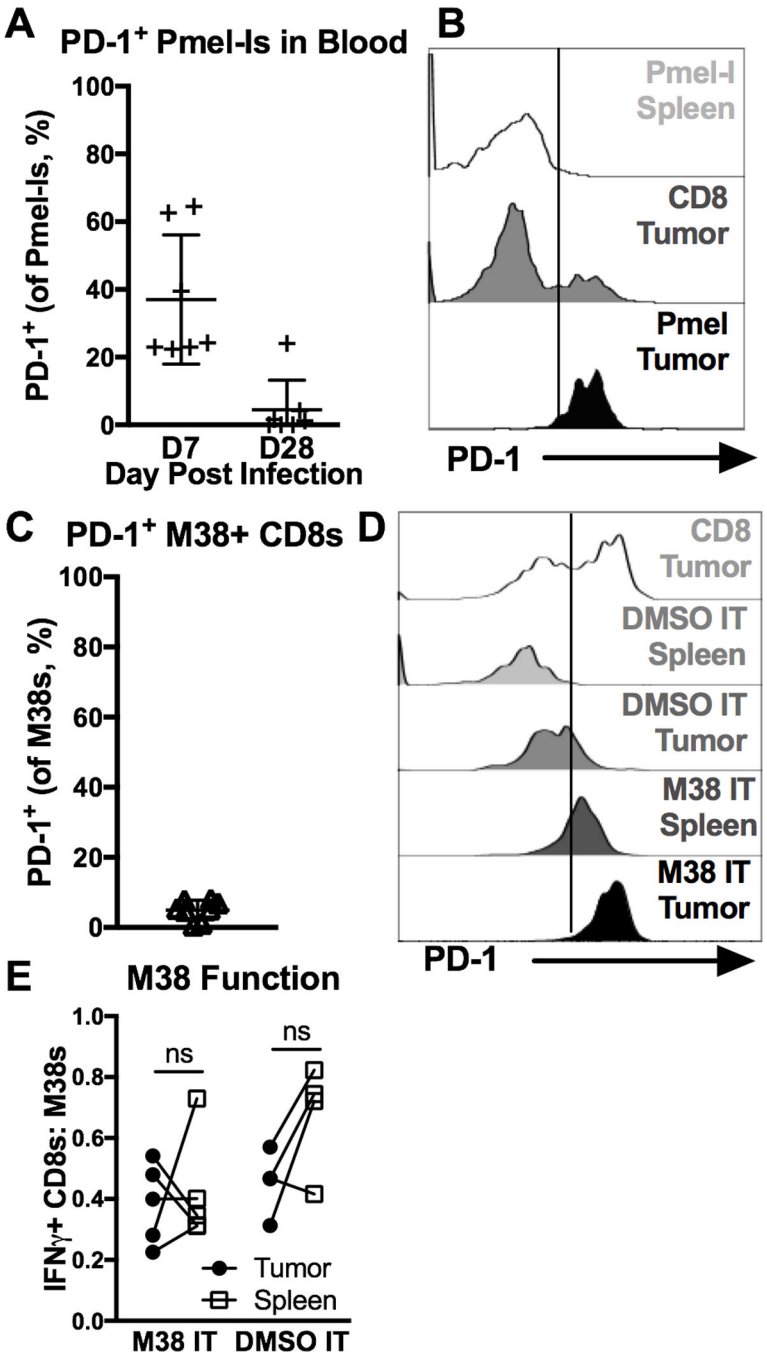

Figure 7. PD-1 is a marker of recent antigen stimulation on TAA-specific and virus-specific CD8$^+$ TIL

A–B) Animals received 10^4 Pmel-Is on D-1, were infected with MCMV-gp100 on D0, given B16F0s on D30 or 31, and sacrificed when tumors were ~40mm^2 (D14–39, n=6, 2 experiments). Shown is (A) the percent PD-1$^+$ Pmel-Is in the blood D7 and D28 post infection (before tumor implantation), and (B) the MFI of PD-1 expression on total and TAA-specific CD8$^+$ T cells (Pmel-Is) in the tumor and spleen at sacrifice. FACS plots of CD8$^+$ T cells in the spleen include both CD8α IV positive and negative cells while T cells in the tumor tissue include only the CD8α IV negative subset. C-F) Mice infected for 30 days

with WT-MCMV were given B16F0s. When tumors were ~20 mm^2 they were intratumorally (IT) injected with M38 peptide in PBS (n=5) or DMSO in PBS (n=4), and sacrificed 7 days later (3 experiments). Shown is (C) the percent of PD-1^+ M38-specific $CD8^+$ T cells in the blood before tumor implantation, (D) the MFI of PD-1 expression on total and M38-specific $CD8^+$ T cells D7 after IT injections, and (E) the functionality of M38-specific T cells in the tumor and spleen assessed as in Fig. 3B on D7 after IT injections. FACS plots of PD-1 expression in the spleen include both CD8α IV positive and negative cells while T cells in the tumor tissue include only the CD8α IV negative subset. All data is represented as the mean +/− SD and the significance (E) was assessed by paired t-tests, $p < 0.05$ = *.

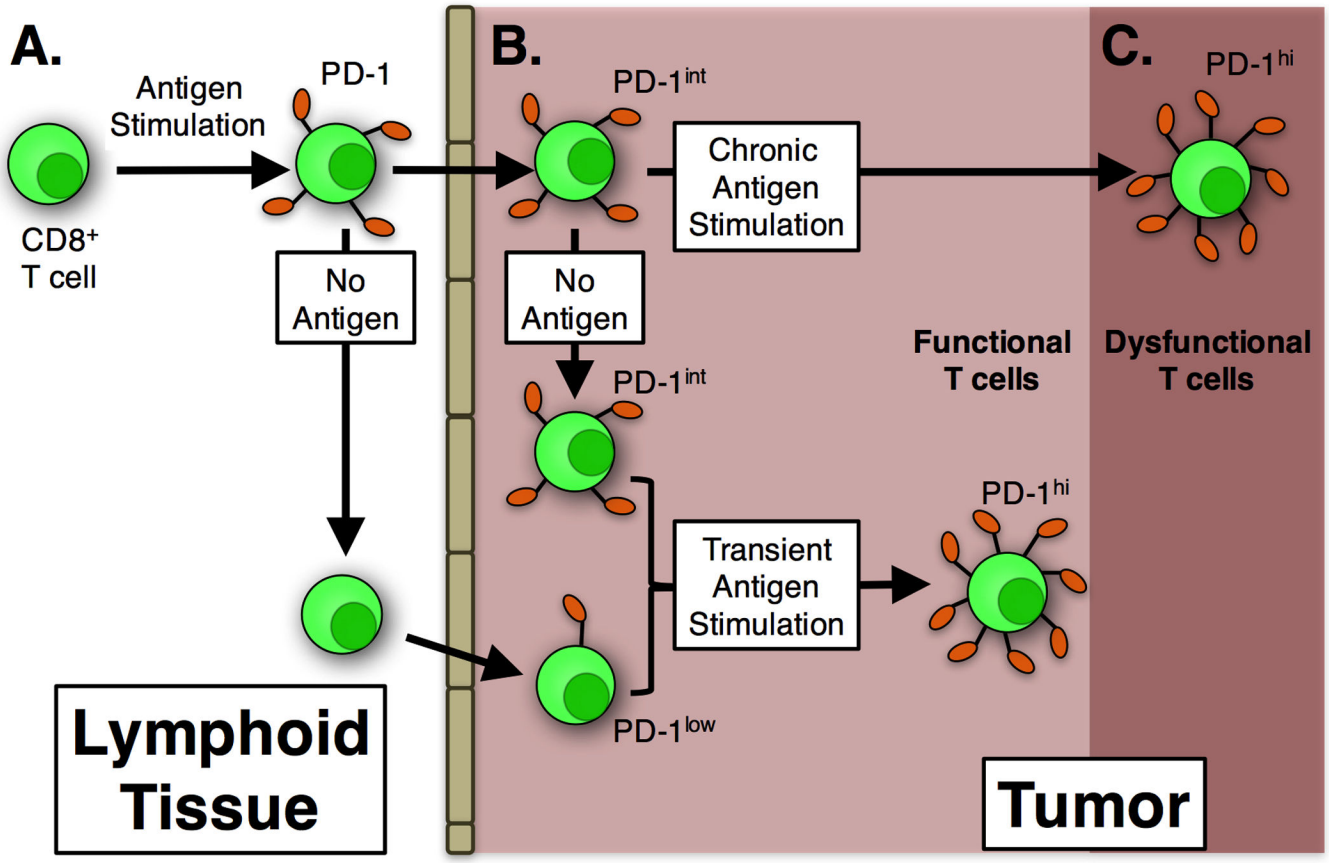

Figure 8. Model of CD8$^+$ T cell infiltration, PD-1 expression, and functionality in melanoma tumors

A) In the lymphoid tissue (and blood), virus-specific CD8$^+$ T cells that are stimulated express PD-1 during clonal expansion but remained functional (Figs 3 and 7). After the acute phase of infection, activated T cells lost PD-1 expression as expected (Figs 3 and 7). B) Some virus-specific CD8$^+$ T cells infiltrated melanoma lesions. If they were PD-1$^+$ upon entry (for example, shortly after clonal expansion), they maintained PD-1 expression at intermediate levels in the tumor environment, but remained functional (Figs 3 and 4). Nevertheless, PD-1 expression on these virus-specific T cells was lower than TAA-specific T cells in the same tumor (Fig 6). If CD8$^+$ T cells had lost PD-1 expression before entering tumors, they remained PD-1^{neg} or became PD-1^{low} in the tumor environment, still remaining functional (Fig 5). Thus, in all cases explored in this study, PD-1 expression on virus-specific T cells was lower than TAA-specific T cells in the same tumor. When virus-specific CD8$^+$ T cells were transiently exposed to antigen in the tumor environment, they upregulated PD-1, but remained functional (Fig 7). C) Chronic antigen stimulation of TAA-specific T cells drove high levels of PD-1 expression and dysfunction.